Superconducting doped topological materials

Satoshi Sasaki[a], Takeshi Mizushima[b,c]

[a]*Institute of Scientific and Industrial Research, Osaka University, Ibaraki, Osaka 567-0047, Japan*
[b]*Department of Materials Engineering Science, Osaka University, Toyonaka, Osaka 560-8531, Japan*
[c]*Department of Physics, Okayama University, Okayama 700-8530, Japan*

Abstract

Recently, the search for Majorana fermions (MFs) has become one of the most important and exciting issues in condensed matter physics since such an exotic quasiparticle is expected to potentially give rise to unprecedented quantum phenomena whose functional properties will be used to develop future quantum technology. Theoretically, the MFs may reside in various types of topological superconductor materials that is characterized by the topologically protected gapless surface state which are essentially an Andreev bound state. Superconducting doped topological insulators and topological crystalline insulators are promising candidates to harbor the MFs. In this review, we discuss recent progress and understanding on the research of MFs based on time-reversal-invariant superconducting topological materials to deepen our understanding and have a better outlook on both the search for and realization of MFs in these systems. We also discuss some advantages of these bulk systems to realize MFs including remarkable superconducting robustness against nonmagnetic impurities.

Keywords: superconducting doped topological materials; $Cu_xBi_2Se_3$; $Sn_{1-x}In_xTe$;$(Pb_{0.5}Sn_{0.5})_{1-x}In_xTe$; $Cu_x(PbSe)_5(Bi_2Se_3)_6$.

1. Introduction

Majorana fermions (MFs) are neutrinos whose property is that particles are their own anti-particles. The existence of MF was initially predicted in high energy physics, but has not been experimentally proved yet [1, 2]. Recently, it has been predicted that the MFs can emerge in topological superconductor (TSC) as gapless excitations [3, 4] that are not electrons or holes but Bogoliubov quasiparticles formed by bound state due to the superposition of electrons and holes [2]. The gapless surface or edge state within the bulk superconducting gap, regardless of whether or not it is fully gapped or partially gapped with nodes [5], is essentially an Andreev bound state (ABS). It is topologically protected since its quantum-mechanical wave function has nontrivial topology. After the theoretical prediction, the search for the MFs in condensed matter physics has become of great interest [2, 6, 7, 8, 9, 10, 11, 12, 13, 14, 15, 16, 17, 18, 19, 20, 21, 22, 23, 24, 25, 26, 27] because, if discovered, MFs will deepen our understanding of quantum states of matter in physics and foster innovations in future quantum technologies. Furthermore, the discovery would provide us a clue to answer what made it difficult for us to observe MF as a neutrino.

Since recent progress on research of MFs elucidates that the topological superconducting states which harbor MFs can be realized in many different systems [2, 6, 7, 8, 9, 10, 11, 12, 13, 14, 15, 16, 17, 18, 19, 20, 21, 22, 23, 24, 25, 26, 27], it would be useful to look over the prerequisites for realizing TSCs. In this review, we focus on bulk time-reversal-invariant superconductors (SCs) derived from degenerately-doped topological materials that are considered to be a promising platform, namely superconducting doped topological insulators (STIs), superconducting doped topological crystalline insulators (STCIs), or superconducting heterostructure materials based on doped topological insulators (TIs). We will describe advantages/disadvantages of those systems that can be distinguished from others in the properties of normal states or symmetry invariance. In particular, it is important to notice that theoretically the superconducting state in the superconducting doped topological materials is robust against non-magnetic impurities [28, 29, 30, 31]. Hence, the doped non-magnetic element in topological materials will exert almost no ill effects on the realization of a TSC with odd-parity paring state. This is one of advantages of superconducting doped topological materials making them to be promising candidates for the TSCs.

We discuss the experimental efforts and achievements on the search for MFs in superconducting doped topological materials, candidate materials for time-reversal-invariant TSCs: $Cu_xBi_2Se_3$, $Sn_{1-x}In_xTe$, $(Pb_{0.5}Sn_{0.5})_{1-x}In_xTe$, and $Cu_x(PbSe)_5(Bi_2Se_3)_6$ and list the issues to be addressed in future studies.

2. Superconducting topological materials

TSCs are accompanied by quasiparticles that have nontrivial topological properties defined in the momentum space. The quasiparticles are essentially MFs which are responsible for non-local correlation, non-abelian statistics, and Ising magnetic response [2, 3, 4, 14]. One of the concrete examples of TSCs is the superfluid ^{3}He, which has offered a prototypical system to realize various kinds of topological phases, owing to the richness of symmetry [24, 25, 32, 33]. As for SCs, only a few bulk

Email addresses: sasaki@sanken.osaka-u.ac.jp (Satoshi Sasaki), mizushima@mp.es.osaka-u.ac.jp (Takeshi Mizushima)

materials are known as strong candidates for the host of MFs, e.g., Sr_2RuO_4 [34] and some heavy fermion SCs, in particular UPt_3 [35, 36, 37, 38].

One of the keys to realize TSCs and MFs in bulk materials is odd parity pairing that satisfies

$$P\Delta(\boldsymbol{k})P^\dagger = -\Delta(-\boldsymbol{k}), \tag{1}$$

where P is the inversion operator. This indicates that for a single-band system, only spin-triplet pairing can be a candidate for bulk centrosymmetric TSCs and MFs. A sufficient criterion for realizing TSCs in odd-parity pairing was derived in Refs. [9, 10, 11, 39], where the topological property is determined by the number of Fermi surfaces that enclose the time-reversal invariant momenta.

Carrier-doped TIs and topological crystalline insulators (TCIs) which we mainly consider in this paper can offer a promising platform to realize TSCs and MFs for the following two reasons: First, owing to the orbital degrees of freedom of electrons embedded in TIs, odd-parity pairing that satisfies Eq. (1) can be realized even in an s-wave channel of Cooper pairs, as a spin-triplet s-wave orbital-singlet, which can be favored by phonon-mediated pairing mechanism. All the odd-parity pairings in doped TIs satisfy a sufficient criterion for realizing TSCs [9, 10, 11, 39]. Second, contrary to conventional wisdom, it has been predicted that a strong spin-orbit coupling makes bulk odd parity superconductivity robust against nonmagnetic disorder [28, 30, 31]. Hence, carrier-doped TIs can expand the horizons of the research field of topological superconducting materials.

In this section, we give an overview of TSCs and time-reversal-invariant TIs as their host materials. Special focus is placed on $Cu_xBi_2Se_3$ as a promising candidate for TSCs. We also make a brief overview on the robustness of bulk odd-parity pairing against disorders [28, 30, 31]. In this paper, we introduce the Pauli matrices in the spin, orbital, and particle-hole spaces, s_μ, σ_μ, and τ_μ, respectively. The repeated Greek indices imply the sum over x, y, z and we set $\hbar = 1$.

2.1. $\mathbb{Z}_2$ TIs and Dirac fermions

To clarify the topological properties of the parent material of STIs, we here start to summarize the discrete symmetries relevant to TIs. Since many time-reversal-invariant TIs hold the inversion symmetry as well as the time-reversal symmetry [40], the Bloch Hamiltonian, $\mathcal{H}_{\rm TI}(\boldsymbol{k})$, satisfies the following relations,

$$P\mathcal{H}_{\rm TI}(\boldsymbol{k})P^\dagger = \mathcal{H}_{\rm TI}(-\boldsymbol{k}), \tag{2}$$

$$\mathcal{T}\mathcal{H}_{\rm TI}(\boldsymbol{k})\mathcal{T}^{-1} = \mathcal{H}_{\rm TI}(-\boldsymbol{k}), \tag{3}$$

where $P = \sigma_x$ and $\mathcal{T} = is_yK$ are the inversion and time-reversal operators, respectively (K is the complex conjugation operator). The symmetry (3) indicates that the eigenstates of the Bloch Hamiltonian, $|u_n^{(0)}(\boldsymbol{k})\rangle$, have Kramers degenerate partners, $|u_n^{(0)}(-\boldsymbol{k})\rangle = \mathcal{T}|u_n^{(0)}(\boldsymbol{k})\rangle$.

It is further natural to suppose that $\mathcal{H}_{\rm TI}(\boldsymbol{k})$ holds a mirror symmetry and N-fold rotation symmetry about the $\hat{\boldsymbol{z}}$-axis, because the discrete symmetries originate in crystalline symmetry relevant to TIs:

$$M\mathcal{H}_{\rm TI}(\boldsymbol{k})M^\dagger = \mathcal{H}_{\rm TI}(-k_x, k_y, k_z), \tag{4}$$

$$U_N\mathcal{H}_{\rm TI}(\boldsymbol{k})U_N^\dagger = \mathcal{H}_{\rm TI}(R_N\boldsymbol{k}), \tag{5}$$

Without loss of generality, the mirror reflection plane is set to be normal to the $\hat{\boldsymbol{x}}$-axis, where the mirror operator $M = is_x$ changes $\boldsymbol{k}$ and $\boldsymbol{s}$ to $(-k_x, k_y, k_z)$ and $(s_x, -s_y, -s_z)$. The SU(2) matrix $U_N = \exp(-i\varphi s_z/2)$ describes the N-fold spin rotation about the $\hat{\boldsymbol{z}}$-axis by an angle $\varphi = 2\pi/N$ ($N \in \mathbb{Z}$) and R_N is the corresponding SO(3) rotation matrix.

Owing to Kramers degenerate band structure, a minimal model for time-reversal-invariant TIs is a 4×4 hermitian matrix. A generic form which holds the symmetries (2) and (3) can be expanded in terms of the five Dirac γ-matrices as $\mathcal{H}_{\rm TI}(\boldsymbol{k}) = d_0(\boldsymbol{k}) + \sum_j d_j(\boldsymbol{k})\gamma_j$ [41, 42]. Following Ref. [40], we take the γ-matrices as $(\gamma_1, \gamma_2, \gamma_3, \gamma_4, \gamma_5) = (\sigma_x, \sigma_y, \sigma_z s_x, \sigma_z s_y, \sigma_z s_z)$. The symmetries (2) and (3) guarantee that all the coefficients are real and that $d_a(\boldsymbol{k})$ is even on $\boldsymbol{k}$ for $a = 0, 1$ and odd otherwise. The discrete symmetries (4) and (5) further constraints $\mathcal{H}_{\rm TI}(\boldsymbol{k})$ in the lowest order on k as

$$\mathcal{H}_{\rm TI}(\boldsymbol{k}) = c(\boldsymbol{k}) + m(\boldsymbol{k})\sigma_x + v_z k_z \sigma_y + v(\boldsymbol{k} \times \boldsymbol{s})_z \sigma_z, \tag{6}$$

where $c(\boldsymbol{k}) = c_0 + c_1 k_z^2 + c_2(k_x^2 + k_y^2)$ and $m(\boldsymbol{k}) = m_0 + m_1 k_z^2 + m_2(k_x^2 + k_y^2)$. The Hamiltonian (6) describes the low-energy band structure of topological materials, including Bi_2Se_3 (TI) [43, 44], SnTe (TCI) [45, 46, 47]. We also notice that as the lowest order correction to Eq. (6), the effect of the "warping" term, $(k_+^3 + k_-^3)\sigma_z s_z$, was discussed in TIs [48] and SCs [49], where $k_\pm \equiv k_x \pm ik_y$.

The topology of the parent material is characterized by the $\mathbb{Z}_2$ invariant, ν [40, 50], which originates in the Berry phase of $|u_n^{(0)}(\boldsymbol{k})\rangle$. The inversion symmetry (2) simplifies the formula for the $\mathbb{Z}_2$ number as $(-1)^\nu = \prod_i \xi(\boldsymbol{\Lambda}_i)$, where $\xi(\boldsymbol{\Lambda}_i) = \pm 1$ is an eigenstate of P at time-reversal-invariant momenta $\boldsymbol{\Lambda}_i$ that satisfy $[\mathcal{T}, \mathcal{H}_{\rm TI}(\boldsymbol{\Lambda}_i)] = 0$. For the form of the Hamiltonian (6), the topological invariant ν is nontrivial (odd) when $\mathrm{sgn}(m_0 m_1) < 0$. Even in the case that ν is trivial, however, another topological number, the Chern number, can be introduced in a mirror symmetric plane of the Brillouin zone [51, 46]. A nonzero mirror Chern number defines *topological crystalline insulators*. As will be discussed in Sec. 3.2, the concrete example is SnTe, which is accompanied by gapless states on the (001) surface, even though the $\mathbb{Z}_2$ number is trivial.

One of the remarkable consequences of an odd ν is the emergence of topologically protected Dirac fermions that are bound at the surfaces. The wave function of Dirac fermions on the surface ($z = 0$) is obtained by solving the equation, $[\mathcal{H}_{\rm TI}(k_x, k_y, -i\partial_z) - \mu]\boldsymbol{\varphi}_{\rm D}(z) = \varepsilon(k_x, k_y)\boldsymbol{\varphi}_{\rm D}(z)$, with a boundary condition $\boldsymbol{\varphi}_{\rm D}(0) = \boldsymbol{0}$. The wave function with the linear dispersion, $\varepsilon(k_x, k_y) = \pm v\sqrt{k_x^2 + k_y^2}$, is given for $c_1 = c_2 = 0$ as

$$\boldsymbol{\varphi}_{\rm D}(z) = (e^{-\kappa_- z} - e^{-\kappa_+ z}) \begin{pmatrix} 0 \\ 1 \end{pmatrix}_\sigma \otimes u_s(k_x, k_y), \tag{7}$$

where $\kappa_\pm = v_z/2m_1 \pm \sqrt{(m_0 + m_2 k_\parallel^2)/m_1 + (v_z/2m_1)^2}$ and $(0, 1)_\sigma^{\rm T}$ is the spinor in the orbital space ($A^{\rm T}$ denotes the transpose of

a matrix A). The spinor u_s in the spin space is determined by $(k_x s_y - k_y s_x)u_\pm = \pm k_\parallel u_\pm$. The penetration depth of the Dirac cone, ℓ, is defined as $\ell \equiv \kappa_-^{-1}$. The surface Dirac fermions in Eq. (7) are fully polarized in the orbital space. In Sec. 4.1, we will discuss the effect of the orbitally polarized Dirac fermions on bulk superconductivity.

2.2. Topology in superconducting topological materials

To derive a sufficient condition for realizing topological superconductivity in doped topological materials, let us here overview the topological invariants, $\mathbb{Z}$ and $\mathbb{Z}_2$ numbers, relevant to time-reversal-invariant SCs. The topological invariant is usually introduced by the global structure of the wave functions of quasiparticles that have a fully gapped excitation spectrum. Such a gapped SC with time-reversal symmetry is categorized to the class DIII in the Altland and Zirnbauer (AZ) table [6, 52], and the topologically non-trivial property in three-dimension is characterized by a $\mathbb{Z}$ topological number, i.e., a winding number. As clarified in Ref. [39], however, topological invariant can be introduced even in a SC having nodal structures. In this case, the $\mathbb{Z}$ is an ill-defined number due to an ambiguity for redefining the superconducting gap, while a $\mathbb{Z}_2$ that corresponds to the parity of the winding number remains as a well-defined number.

The quasiparticle states that characterize topological superconductivity are obtained by solving the Bogoliubov-de Gennes (BdG) Hamiltonian in the particle-hole space,

$$\mathcal{H}(\boldsymbol{k}) = \begin{pmatrix} \mathcal{H}_{\rm TI}(\boldsymbol{k}) - \mu & -i\Delta(\boldsymbol{k})s_y \\ is_y\Delta^\dagger(\boldsymbol{k}) & -\mathcal{H}_{\rm TI}^{\rm T}(-\boldsymbol{k}) + \mu \end{pmatrix}, \tag{8}$$

where μ is the chemical potential. In superconducting states, the particle sector is coherently coupled to the hole sector through the pair potential $\Delta(\boldsymbol{k})$. Here, we concentrate our attention on time-reversal-invariant SCs that satisfy $\mathcal{T}\Delta(\boldsymbol{k})\mathcal{T}^{-1} = \Delta(-\boldsymbol{k})$. The BdG Hamiltonian, then, holds the time-reversal symmetry, $\mathcal{T}\mathcal{H}(\boldsymbol{k})\mathcal{T}^{-1} = \mathcal{H}(-\boldsymbol{k})$, and the particle-hole symmetry, $C\mathcal{H}(\boldsymbol{k})C^{-1} = -\mathcal{H}(-\boldsymbol{k})$ with $C = \tau_x K$. Combining these symmetries, one can define the chiral operator Γ, which is anti-commutable with $\mathcal{H}(\boldsymbol{k})$,

$$\{\Gamma, \mathcal{H}(\boldsymbol{k})\} = 0, \quad \Gamma = -iC\mathcal{T}. \tag{9}$$

The discrete symmetries with $\mathcal{T}^2 = -1$, $C^2 = +1$, and $\Gamma^2 = +1$ categorize this system to the DIII class in the AZ table [6, 52].

The topological properties of superfluids and SCs are generally determined by the global structure of the Hilbert space spanned by the eigenvectors of the occupied band, $|u_n(\boldsymbol{k})\rangle$ obtained from $\mathcal{H}(\boldsymbol{k})|u_n(\boldsymbol{k})\rangle = E_n(\boldsymbol{k})|u_n(\boldsymbol{k})\rangle$. To capture the topological property, it is convenient to introduce the so-called Q-matrix, $Q(\boldsymbol{k}) = \sum_{E_n>0}|u_n(\boldsymbol{k})\rangle\langle u_n(\boldsymbol{k})| - \sum_{E_n<0}|u_n(\boldsymbol{k})\rangle\langle u_n(\boldsymbol{k})|$ [6, 52]. Since the traceless Q-matrix satisfies the conditions, $Q^2(\boldsymbol{k}) = +1$, the Q-matrix continuously flattens the eigenvalues of $\mathcal{H}(\boldsymbol{k})$ to -1 (occupied) and $+1$ (unoccupied). Therefore, the Q-matrix maps the Brillouin zone onto the target space spanned by the eigenvectors of the BdG Hamiltonian. The chiral symmetry is still preserved by the Q-matrix, $\{\Gamma, Q(\boldsymbol{k})\} = 0$, which is crucial for introducing topological invariant. In the basis that Γ is diagonalized to $\Gamma = \mathrm{diag}(+1, -1)$, the Q-matrix becomes off-diagonal and is reduced to $q(\boldsymbol{k}) \in \mathrm{U}(N)$. Hence, the relevant homotopy group for the projector $Q(\boldsymbol{k})$ in three dimensions is given by $\pi_3[\mathrm{U}(N)] = \mathbb{Z}$. The topological invariant is defined as the three-dimensional winding number [6, 52, 53],

$$w_{\rm 3d} = -\int \frac{d\boldsymbol{k}}{48\pi^3}\epsilon_{\mu\nu\eta}\mathrm{tr}\left[\Gamma(Q\partial_\mu Q)(Q\partial_\nu Q)(Q\partial_\eta Q)\right]. \tag{10}$$

For the DIII class, $w_{\rm 3d}$ can be an arbitrary integer value, which guarantees the existence of a surface Majorana cone [6, 7, 54].

As clarified in Refs. [10, 11, 39], the $\mathbb{Z}_2$ number that characterizes the parity of $w_{\rm 3d}$ determines a sufficient criterion for realizing time-reversal-invariant TSCs. Here, we suppose an odd-parity pairing that satisfies Eq. (1). This ensures that the BdG Hamiltonian holds the inversion symmetry up to the $\pi/2$ phase rotation,

$$\mathcal{P}\mathcal{H}(\boldsymbol{k})\mathcal{P}^\dagger = \mathcal{H}(-\boldsymbol{k}), \tag{11}$$

where $\mathcal{P} = P\tau_z$. The inversion symmetry simplifies the parity of $w_{\rm 3d}$ to [10, 11, 39]

$$(-1)^{w_{\rm 3d}} = \prod_{i,m}\mathrm{sgn}\left[\varepsilon_{2m}(\boldsymbol{\Lambda}_i)\right], \tag{12}$$

where $\varepsilon_m(\boldsymbol{\Lambda}_i)$ is the energy dispersion of the normal state at time-reversal invariant momenta, which is obtained as the eigenvalues of $\mathcal{H}_{\rm TI}(\boldsymbol{\Lambda}_i) - \mu$ with the chemical potential μ. Owing to the time-reversal symmetry, the energy band of carrier-doped TIs has a Kramers pair as $\varepsilon_{2m}(\boldsymbol{\Lambda}_i) = \varepsilon_{2m+1}(\boldsymbol{\Lambda}_i)$.

The $\mathbb{Z}_2$ number in odd parity SCs was first introduced by Sato [9] in the case of a single-band system and extended to a general case by Sato [11] and Fu and Berg [10], independently. Equation (12) indicates that the mod-2 winding number is determined by counting the number of Fermi surfaces enclosing $\boldsymbol{k} = \boldsymbol{\Lambda}_i$. The topological invariant is non-trivial, i.e., $(-1)^{w_{\rm 3d}} = -1$, when the number of the Fermi surfaces is odd, and trivial otherwise, $(-1)^{w_{\rm 3d}} = +1$. Hence, odd-parity pairing and the shape of the Fermi surfaces at time-reversal-invariant momenta are sufficient conditions for realizing topological superconductivity and helical MFs in doped TIs.

Both the $\mathbb{Z}$ and $\mathbb{Z}_2$ numbers require the quasiparticle excitation to be fully gapped, i.e., $\det\mathcal{H}(\boldsymbol{k}) \neq 0$. For time-reversal-invariant nodal SCs, however, the node structure is not topologically protected and removed by introducing a small perturbation δ that transforms Δ to open a finite gap at the nodal points without breaking the time-reversal symmetry [39]. The unambiguously-defined δ is set to be $\delta \to 0$ after the $\mathbb{Z}_2$ (not $\mathbb{Z}$) topological invariant is evaluated. This simple procedure enables to define the topological numbers in nodal SCs.

2.3. Topological odd parity superconductivity in doped TIs (TCIs)

Since orbital degrees of freedom is inherent to the parent material of STIs, a Cooper pair potential realized in STIs has orbital degrees of freedom in addition to the spin and momentum dependence. Therefore, a general form of the pair potential in bulk STIs is given by $(i\Delta s_y)_{s_1s_2,\sigma_1\sigma_2}(\boldsymbol{k})$, where

(s_1, s_2) and (σ_1, σ_2) refere to spin and orbital indices of paired particles, respectively. In general, the Fermi-Dirac statistics requires the pair potential to be odd under the exchange of relative coordinates, and orbital states, $(i\Delta s_y)_{s_1 s_2, \sigma_1 \sigma_2}(\boldsymbol{k}) = -(i\Delta s_y)_{s_2 s_1, \sigma_2 \sigma_1}(-\boldsymbol{k})$. For s-wave channel, this condition reduces to

$$\Delta = s_y \Delta^{\mathrm{T}} s_y. \tag{13}$$

Here, we suppose even-frequency superconductivity as the bulk pairing of STIs [4]. In single-band SCs, the condition is satisfied only by spin-singlet even parity pairing states. Owing to orbital degrees of freedom inherent to the parent material of STIs, however, odd parity pairing can be realized even in s-wave channel, when the conditions (1) and (13) are satisfied.

Let us now specify the possible s-wave pairing symmetry that satisfies the conditions (1) and (13) for realizing odd parity superconductivity. For spin singlet pairing, the pair potential Δ that satisfies Eq. (13) is generally parameterized with a vector $\boldsymbol{d}^{(\mathrm{s})}$ in the orbital space as $\Delta = i\sigma_\mu \sigma_y d_\mu^{(\mathrm{s})}$, which is the spin-singlet even-parity orbital-triplet state. Among the possible orbital-triplet states, only the pairing, $\Delta = i\sigma_x \sigma_y d_x^{(\mathrm{s})} \propto \sigma_z$, can be odd parity pairing. A general form of spin triplet s-wave pairing is obtained as $\Delta = i s_y s_\mu d_\mu^{(\mathrm{t})}$, with a vector in the spin space, $\boldsymbol{d}^{(\mathrm{t})}$. This pairing symmetry categorized to the spin-triplet even-parity orbital-singlet state always satisfies the odd-parity condition in Eq. (1).

In Table 1, we summarize possible s-wave pairing symmetries in STIs with the rhombohedral D_{3d} crystalline symmetry [10, 39, 55, 56], which are relevant to both $Cu_xBi_2Se_3$ and $Sn_{1-x}In_xTe$ (See Sec. 3.1 and 3.2). There are six independent matrices, $(\Delta_{1a}, \Delta_{1b}\sigma_x, \Delta_2\sigma_y s_z, \Delta_3\sigma_z, \Delta_{4x}\sigma_y s_x, \Delta_{4y}\sigma_y s_y)$, that satisfy the criterion (13) for the Fermi-Dirac statistics, where Δ_j (j: 1a, 1b, 2, 3, 4x, and 4y) denote the amplitude of each pair potential. Their gap structures are also summarized in Table 1, where $(\Delta_{1a}, \Delta_{1b}\sigma_x)$ and $\Delta_2\sigma_y s_y$ are fully gapped and the others are accompanied by point nodes [56, 57]. We notice that full gap can be realized in the E_u state (see Sec. 4.1). As mentioned above, all odd parity pairing states can be topologically nontrivial, regardless of nodal structures, when the time-reversal-invariant momentum $\boldsymbol{\Lambda} = \boldsymbol{0}$ is enclosed by the Fermi surface.

A direct consequence of topological odd parity superconductivity is the existence of gapless surface states. The surface structure and tunneling spectroscopy of STIs have been studied theoretically [55, 58, 59, 60, 61]. The A_{2u} and E_u states in Table 1, which are topological odd parity pairing with point nodes, are accompanied by zero energy flat bands connecting two point nodes that are bound to the surface. We will illustrate in Sec. 4.2 that the zero energy flat band is protected by the hidden $\boldsymbol{Z}_2$ symmetry that is obtained by combining the mirror symmetry and time-reversal symmetry. Based on well-established wisdom in unconventional SCs [62, 63], the symmetry-protected surface Fermi arc is responsible for a pronounced zero-bias conductance peak in tunneling spectroscopy.

The A_{1u} state is similar to the Balian-Werthamer (BW) state realized in the superfluid ^{3}He which is a concrete example of time-reversal-invariant TSCs with a full gap [6, 7, 24, 25, 32].

Δ	Gap	Inversion	Mirror	Topology	Γ
Δ_{1a}, $\Delta_{1b}\sigma_x$	full	+	+	–	A_{1g}
$\Delta_2\sigma_y s_z$	full	–	–	$\mathbb{Z}$	A_{1u}
$\Delta_3\sigma_z$	point	–	+	$\mathbb{Z}_2$	A_{2u}
$\Delta_{4x}\sigma_y s_x$	point	–	+	$\mathbb{Z}_2$	E_u
$\Delta_{4y}\sigma_y s_y$	full	–	–	$\mathbb{Z}$	E_u

Table 1: Pairing potentials in STIs, gap structures, and their parity under inversion P and mirror reflection $M = is_x$: Γ denotes the representation of the D_{3d} symmetry. Note that a full gap behavior in the E_u state is discussed in Sec. 4.1.

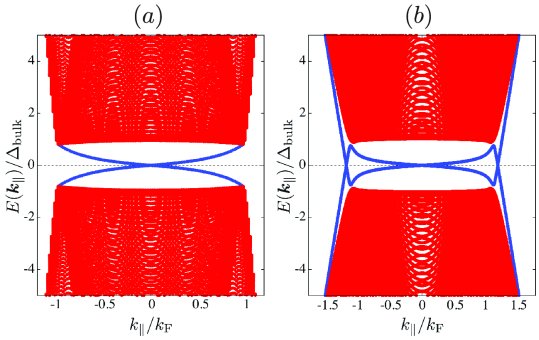

Figure 1: Energy spectra of the A_{1u} state: The "cone" shape of the surface bound states (blue curve) for $(m_1 m_0/v_z^2, m_2 m_0/v_z^2) = (-0.59, -0.20)$ (a) and the "caldera" shape for $(-0.17, -0.20)$ (b), where Δ_{bulk} and k_{F} denote the bulk excitation gap and Fermi momentum, respectively.

The BW state is accompanied by the gapless surface state having a linear dispersion, which is called the Majorana cone. The resultant tunneling conductance of the BW state always shows a double-peak structure, rather than a zero-bias conductance peak [64]. However, it has recently been pointed out [55, 59] that the dispersion of gapless surface states twists at finite momenta $k_\parallel \equiv \sqrt{k_x^2 + k_y^2}$ which is parallel to the surface. The velocity of the Majorana cone near $\boldsymbol{k}_\parallel = \boldsymbol{0}$, $\tilde{v}_{\mathrm{surf}}$, is given with the parameters in $\mathcal{H}_{\mathrm{TI}}(\boldsymbol{k})$ as [55, 59]

$$\tilde{v}_{\mathrm{surf}} = \frac{1 - \sqrt{1 + 4\tilde{m}_1 + 4\tilde{m}_1^2\tilde{\mu}^2}}{2\tilde{m}_1\tilde{\mu}^2} \frac{v\Delta}{m_0}, \tag{14}$$

where $\tilde{m}_1 \equiv m_0 m_1 / v_z^2$. At the critical velocity that satisfies $\tilde{v}_{\mathrm{surf}} = 0$, the topological surface state undergoes a structural transition from a "cone" (Fig. 1(a)) to "caldera" shape (Fig. 1(b)) [55].

In Fig. 1(b), additional crossings of the dispersion of the surface state appear around $k_\parallel \sim k_{\mathrm{F}}$. The crossing is attributed to the cooperative effect of a remnant of the surface Dirac fermions in the parent TI and the surface MFs [55, 59]. Let us suppose the situation that the Dirac cone is well isolated from the conduction band, which corresponds to the situation with low μ values. This is relevant to $Cu_xBi_2Se_3$, where well-defined Dirac cone was observed by angle resolved photoemission spectroscopy (ARPES) [65] at the Fermi level. Therefore, the low energy structure is regarded as an effective two-channel model that is composed of the conduction band electrons and Dirac fermions. The conduction band opens a superconducting gap when adding $\Delta_2\sigma_y s_z$, while the dispersion of the surface Dirac fermions re-

main gapless near the Fermi energy [58, 66]. Hence, the dispersion (14) of the MFs emergent around $\boldsymbol{k} = \boldsymbol{0}$ must smoothly connect to the dispersion of the gapless Dirac fermions. The cooperative effect of surface Majorana and Dirac fermions necessarily gives rise to the twisting of surface Majorana cone and results in a caldera structure. For a large μ where the surface Dirac cone merges into the bulk conduction band, the surface states induced by topological odd parity superconductivity remains as a cone shape. The structural transition of the surface bound states occurs in the case of the E_u state as well.

Owing to the structural transition, a pronounced zero-bias conductance peak can be expected not only in the E_u state but also in the A_{1u} state. The A_{1u} state with the caldera shape of surface MFs has a sharp zero energy peak in the surface density of state, which is responsible for the zero-bias conductance peak [55, 59, 60, 67].

2.4. Effect of disorders on bulk odd parity superconductivity

As clarified in Sec. 2.3, odd parity pairing is a sufficient condition for realizing topological superconductivity in doped TIs. Similarly with a conventional *s*-wave pairing, the A_{1g} state in Table 1 is highly insensitive to disorder [68]. Contrary to a conventional *s*-wave pairing, however, *unconventional* superconducting states have been believed to be fragile against disorders. This suggests that unconventional superconductivity can be realized only in clean materials. Since the superconducting doped topological materials typically have a short mean-free path [69], the robustness of odd-parity superconductivity remains an important issue.

Michaeli and Fu [28] recently predicted that in contrast to conventional wisdom, the A_{1u} state, which is one of the odd parity pairings, remains robust against disorder. They found that an approximate chiral symmetry emergent in STIs prevents the superconducting compound from pair decoherence induced by impurity scattering. Similar conclusions were derived in Ref. [30], based on a self-consistent T-matrix approach for impurity scattering. The robustness against disorder was also reported by Nagai [31] in the case of the E_u state which has the odd-parity pairing with point nodes.

3. Candidate materials

The search for topological phases of matter with time reversal symmetry brought about the discovery of TI materials and stimulated the search for an even more exotic state of matter, TSC, a superconducting cousin of TI. Opposed to the ideal TIs, the bulk of existing materials at the early stage of TI research was conductive and smeared the novel properties of the surface states. While achieving a bulk-insulating state in real TI samples has been a great experimental challenge, inducing superconductivity in TI samples by doping carrier proved to be a great experimental challenge as well.

3.1. Electron-doped TI: $Cu_xBi_2Se_3$

$Cu_xBi_2Se_3$, the first example of a superconducting doped TI, is a layered material consisting of stacked Se-Bi-Se-Bi-Se quintuple layers that are only weakly bonded to each other by van der Waals forces. It has the same rhombohedral crystal structure as Bi_2Se_3 ($R\bar{3}m$ space group [69, 70]) with the representation of D_{3d} point group [10]. Its superconductivity arises as a consequence of Cu intercalation into the van der Waals gap of the parent compound Bi_2Se_3 yielding an electron concentration of $\sim 2\times10^{20}$ cm^{-3} with a maximum transition temperature T_c of 3.8 K for $0.12 < x < 0.15$, as well as a metallic behavior of the resistivity in the normal state [70]. The bulk superconductivity of $Cu_xBi_2Se_3$ samples was confirmed by the specific heat measurements which showed that the superconducting state of $Cu_xBi_2Se_3$ for $x \simeq 0.3$ is likely to be fully gapped [69]. The carrier density of order of 10^{20} cm^{-3} is very low for SCs whose maximum T_c is in the order of a few K within the framework of the Bardeen-Cooper-Schrieffer (BCS) theory. The anomalously high T_c for a relatively low carrier density may indicate that the pairing mechanism of the superconducting $Cu_xBi_2Se_3$ could be affected by the strong spin-orbit coupling, albeit still be governed by the electron-phonon mechanism in the same way as most of the existing SCs.

Stimulated by the discovery of superconductivity in doped TI $Cu_xBi_2Se_3$, in 2010, Fu and Berg discussed the possible pairing symmetry within a two-orbital model and a sufficient criterion for realizing time-reversal-invariant TSCs in materials with inversion symmetry [10]. Intriguingly, a novel spin-triplet pairing with odd parity is favored by strong spin-orbit coupling with gapless surface ABSs within a full pairing gap in the bulk: We emphasized in Sec. 2.2 that what is important for TSCs is odd parity pairing (See Eq. (1)) and a nontrivial $\mathbb{Z}_2$number is defined for all odd parity pairing even in nodal SCs.

The discovery of the $Cu_xBi_2Se_3$ SC attracted a lot of attention in the community, however, experimental studies of this material were hindered at the beginning by difficulties of material synthesis. Thanks to employing electrochemical Cu intercalation (ECI) technique combined with the post annealing that is essential for the activation of the superconductivity (a typical sample image of ECI $Cu_xBi_2Se_3$ is displayed in Fig. 2(a)) [69, 71], the maximum shielding fraction of $Cu_xBi_2Se_3$ now can reach up to ~50% at 1.8 K with Cu concentration x of ~0.3; besides, the maximum value can be even larger at lower temperatures. Meanwhile, serious improvements of the melt-grown (MG) synthesis have been done [72, 73, 74]. Currently $Cu_xBi_2Se_3$ has been the most widely studied as a candidate for the TSCs.

It would be prudent to discuss disorder effects in $Cu_xBi_2Se_3$ since odd-parity pairing state in general disfavors disorders [75, 76, 77] as mentioned in Sec.2.4. There is a systematic unbalance between the number of the intercalated Cu atoms and that of the increase in the carrier density [69]. Progressive Cu intercalation into the system introduces significant disorder [70, 71, 73] and an intrinsic inhomogeneity [71], leading to an anomalous suppression of the superfluid density which was deduced from the measurements of the lower critical field [78] and an optical spectroscopic study [79]. At the same time, the transition temperature T_c is monotonously and only moderately suppressed from $T_c \simeq 3.8$ K ($x \simeq 0.1$) to $T_c \simeq 2.6$ K ($x \simeq 0.5$), which agrees with the non-magnetic impurity effect theoretically predicted for this class of TSCs [28, 29, 30, 31].

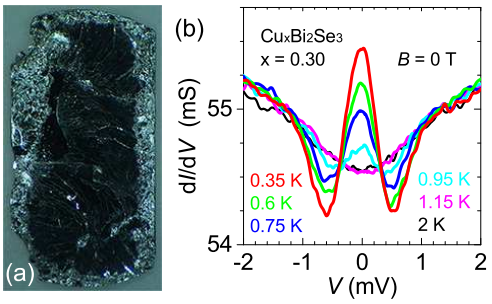

Figure 2: $Cu_xBi_2Se_3$ and zereo-bias conductance peak. (a) A typical cleaved surface image of Cu-intercalated Bi_2Se_3 with post annealing. (b) Point-contact spectra (dI/dV vs bias voltage) of $Cu_xBi_2Se_3$ with $x = 0.3$ for 0.35–2 K measured in 0 T.

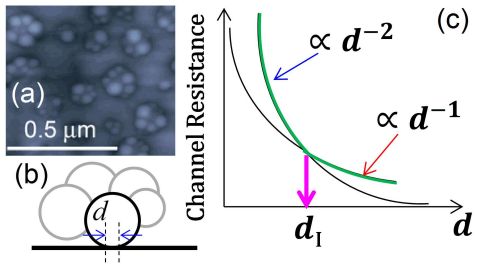

Figure 3: Legitimacy of soft point contact. (a) Atomic force microscope picture of Ag nano grains on the measured surface after the measurement lead is removed. (b) A diameter of the contact area of a nano grain in a Ag cluster at the sample surface. (c) An expected diameter dependence in the resistnace of an electron-transport channel.

The robust topological superconductivity even in disorder can be derived from the relativistic effects in doped topological materials [30, 31].

In order to confirm whether or not a SC is a TSC, it can be useful to verify the existence of an ABS consisting of MFs that is a low-energy gapless excitation at the surface by detecting surface "low-energy" phenomena, in particular electron tunneling. The gapless excitations that create the density of states within the superconducting gap can be detected as a zero-bias conductance peak (ZBCP) in tunneling spectroscopy. Indeed, both the A_{1u} and E_u states in Table 1, which have bulk topological odd parity superconductivity, are responsible for a pronounced ZBCP on the (111) surface of $Cu_xBi_2Se_3$ [55, 59]. It should be mentioned that a ZBCP was observed in Sr_2RuO_4, a strong candidate for time-reversal breaking chiral p-wave TSCs [77, 80].

Actually, the ZBCP was observed by soft point-contact spectroscopy experiments on a cleaved (111) surface of ECI $Cu_xBi_2Se_3$ for $x \simeq 0.3$ with a tiny drop of silver paint consisting of clusters of Ag grains that produce Ag-grain parallel channels at the point contact as shown in Fig. 2(b) [39]. A typical diameter of grains appears to be ~20–50 nm estimated from the image taken by the atomic force microscope in Fig. 3(a) and the diameter of the contact area for one grain d is always smaller than that of the grain size (see Fig. 3(b)). In the case of ballistic electron transport, the resistance of the channel can be estimate as Sharvin resistance that is proportional to $1/d^2$ while in the case that electrons are scattered and loose kinetic energy, the channel resistance can be estimated as Maxwell resistance that is proportional to $1/d$ [81]. The Sharvin resistance becomes dominant when d is smaller than the intersection point $d_{\rm I}$ between two types of resistance with respect to d as indicated in Fig. 3(c), which is ~100 nm in the case of Ag [82]. Since the Ag grain size is smaller than $d_{\rm I}$, the electron transport in the case of the soft point contact can be ballistic, and hence spectroscopy in the presence of a finite repulsive potential barrier at the boundary between the Ag grain and a SC can be performed. Theoretical considerations of all possible superconducting states shows that the observed surface ABS of $Cu_xBi_2Se_3$ is due to MFs [39]. Consistently, similar ZBCPs were observed by other point-contact spectroscopy experiments with Au tip on MG $Cu_xBi_2Se_3$ for $x \simeq 0.25$ [83].

On the contrary, both unconventional ZBCP and conventional Blonder-Tinkham-Klapwijk (BTK) spectra were observed on the surface of MG $Cu_xBi_2Se_3$ for $x \simeq 0.20$ by point-contact spectroscopy with Au tip [74]. Andreev reflection spectroscopy performed by a nanoscale device showed spectra partially fitted by BTK theory [84]. Moreover, a conventional tunneling spectrum was observed on a cleaved surface of ECI $Cu_xBi_2Se_3$ for $x \simeq 0.25$ by scanning tunneling spectroscopy (STS) [85]. These aroused a controversy with respect to the nature of superconductivity in $Cu_xBi_2Se_3$. It is worth noting that recent self-consistent calculations for surface density of states (SDOSs) has clarified this puzzling issue: the surface Dirac fermions in a conventional pairing state of the s-wave SC will open an additional gap larger than the bulk superconducting gap yielding a two-gap structure due to parity mixing of the pair potential near the surface, nonetheless the STS spectra exhibited only single-gap structure. Importantly, the parity mixing is absent in an unconventional pairing state of odd-parity SC [67]. In addition, recent ARPES experiments revealed that the Fermi surface (FS) of superconducting $Cu_xBi_2Se_3$ is a cylindrical open FS [86] coexisting with the topological gapless surface states of Bi_2Se_3 well-separated from the bulk conduction band [65, 86]. Therefore the STS spectra can be originated from topological odd-parity superconductivity with a cylindrical FS [67]. Further details will be discussed in Sec. 4.1.

It is worth mentioning that the pressure variation of the superconducting phase of MG $Cu_xBi_2Se_3$ for $x \simeq 0.3$ was investigated by applying a hydrostatic pressure up to 2.31 GPa [87] and the superconductivity appears to be robust up to 6.3 GPa. The sufficiently large mean free path and the variation of $B_{c2}(T)$ that agrees with the p-wave polar-state model indicate the p-wave spin-triplet superconductivity of $Cu_xBi_2Se_3$, although an anisotropic spin-singlet state cannot be discarded completely. Apparently further studies on $Cu_xBi_2Se_3$ with different measurement techniques are required to elucidate the true nature of this material.

3.2. Hole-doped TCI: $Sn_{1-x}In_xTe$ and $(Pb_{0.5}Sn_{0.5})_{1-x}In_xTe$

Based on a guiding principle suggested from the discovery of $Cu_xBi_2Se_3$, low-carrier-density semiconductors whose Fermi

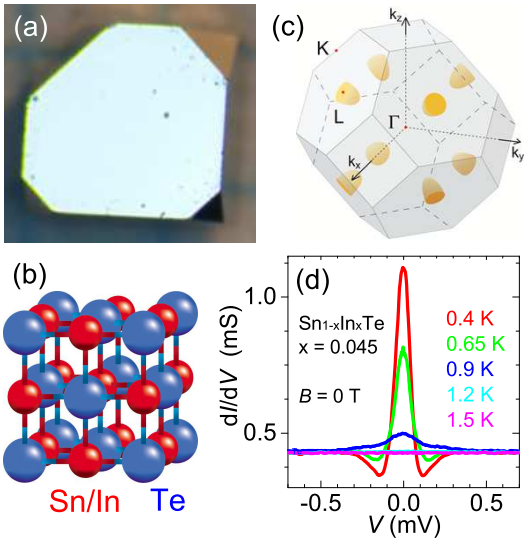

Figure 4: $Sn_{1-x}In_xTe$. (a) A typical facet image of $Sn_{1-x}In_xTe$ crystal grown by the vapor-transport method. (b) Cubic rocksalt crystal structure of $Sn_{1-x}In_xTe$. (c) The Fermi surfaces of p-type SnTe are centered around the four equivalent L points, which belong to the time-reversal-invariant momenta, in the bulk Brillouin zone of the cubic structure with fcc Bravais lattice. (d) Point-contact spectra (Bias-voltage (V) dependence of the differential conductance, $[dI/dV](V)$, at various temperatures) of $Sn_{1-x}In_xTe$ with $x = 0.045$ measured in 0 T.

surfaces are centered around time-reversal-invariant momenta in strong spin-orbit coupling systems, in particular doped TCIs with mirror symmetry, are other likely candidates for TSCs. In-doped SnTe (denoted $Sn_{1-x}In_xTe$), a first example of STCIs, has the same rocksalt crystal structure ($Fm\bar{3}m$ space group) with the representation of O_h point-group symmetry as pristine SnTe (see Fig. 4(b)) at ambient temperature. It reveals a metallic behavior of the resistivity in the normal state in single crystals synthesized in two different ways: Melt growth [88] and vapor-solid growth [89, 90]. A typical faceted single crystal is shown in Fig. 4(a). It has been known that hole-doped SnTe, a degenerately-doped TCI due to Sn vacancies, superconducts and T_c increases as the hole density increases from 0.024 K ($\sim 5\times10^{20}$ cm^{-3}) to ~0.2 K (20×10^{20} cm^{-3}) [91]. When cooled, ferroelectric structural phase transition (SPT) occurs in SnTe so that superconducting degenerately-doped SnTe must have a rhombohedral crystal structure.

Upon substitution of Sn by In, however, T_c jumps as high as ~1 K and gradually increases as the In content increases, suppressing the SPT, although the hole density remains similar [88]. Above $x \sim 0.04$ the SPT is completely suppressed. Nevertheless, the topological surface state of SnTe is preserved on $Sn_{1-x}In_xTe$ for $x = 0.045$ providing evidence for the presence of an inverted band structure as in pristine SnTe [92] and, therefore, $Sn_{1-x}In_xTe$ with a moderate In content is a superconducting doped TCI. Although it has not been clarified yet whether or not $Sn_{1-x}In_xTe$ with very high In content can still be a doped TCI, interestingly, progressive In doping enhances T_c up to 4.5 K for $x = 0.45$ [93] or ~4.8 K for $x = 0.45$ [94] determined by the onset of diamagnetism, and 4.7 K for $x \simeq 0.40$ determined by the onset of superconducting transition in the resistivity measurement [95].

The bulk superconductivity of $Sn_{1-x}In_xTe$ was confirmed by the specific heat measurement for $0.021 < x < 0.12$ [88], $0.025 < x < \sim 0.05$ [96] and $x = 0.4$ [95], as well as muon-spin rotation or relaxation (μSR) measurement for $0.38 < x < 0.45$ [94]. Both measurements show the superconducting state of $Sn_{1-x}In_xTe$ is likely to be fully gapped. The volume fraction of $Sn_{1-x}In_xTe$ is essentially 100%. The absence of impurity phase is an advantage of this material over $Cu_xBi_2Se_3$, if this is really a TSC.

It turns out that the superconducting state of $Sn_{1-x}In_xTe$ has a rich phase diagram where the dependence of T_c on indium content x below ~0.04 (in the ferroelectric rhombohedral phase) in vapor-grown (VG) single crystals [96] appears to be different from that in MG single crystals [88]. The different trend of T_c can be explained by the unusual role of impurity scattering within the framework of the BCS theory based on the Martin-Phillips theory for the enhancement of T_c [96] implying that the strength of the impurity scattering in crystals is probably different when grown in different ways. Hence, the superconducting state of $Sn_{1-x}In_xTe$ in the ferroelectric rhombohedral phase is not necessarily unconventional and can be topologically trivial with conventional even-parity pairing.

Importantly, the ZBCP, signature of the surface ABS was observed by the soft point-contact spectroscopy on VG $Sn_{1-x}In_xTe$ single crystals for $x = 0.045$ as plotted in Fig. 4(d)[89], indicating the realization of a topological superconducting state in the cubic phase. To identify the nature of the superconducting state in $Sn_{1-x}In_xTe$, the conduction and valence bands in the vicinity of four L points of the fcc Brillouin zone, where ellipsoidal Fermi surfaces in the normal state are located as drawn in Fig. 4(c), are described by the $k \cdot p$ Hamiltonian in Eq. (6) [46]. The effective Hamiltonian of $Sn_{1-x}In_xTe$ has essentially the same form and the same symmetry classification of the possible gap functions as that of $Cu_xBi_2Se_3$ except for the presence of the threefold rotation symmetry around (111) axis in $Sn_{1-x}In_xTe$. Theoretical considerations lead to the conclusion that all possible superconducting states are topologically nontrivial [89].

However, even in the cubic phase, no clear bulk unconventionality was observed in $Sn_{1-x}In_xTe$ crystals with a very high In content so far [93, 94, 95]. It is worth noting that the recent numerical calculations using a self -consistent T-matrix approach in the case of k-independent pairing reveal that the superconducting state can be altered from p- (odd-parity pairing) to s-wave (even -parity pairing) character depending on the magnitude of the relativistic effects in the normal-state Dirac Hamiltonian of three-dimensional TSCs [30, 31]. In this regard, s-wave superconductivity which is robust against a strong impurity scattering would dominate the superconducting state of high-In-content samples where μ is separated from the Dirac points. Hence, the odd-parity state can be realized only in the lowest T_c samples in the cubic phase where μ is close to the Dirac points and the impurity scattering is the weakest, though the surface states are significantly broadened due to strong quasiparticle scattering caused by In doping [92].

Recently the effect of the In concentration on the crystal

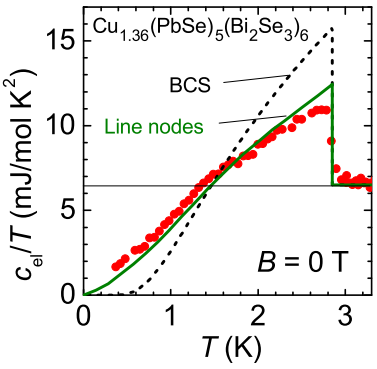

Figure 5: Specific heat of $Cu_x(PbSe)_5(Bi_2Se_3)_6$. Superconducting transition in c_{el}/T in 0 T obtained after subtracting the phonon contribution determined in 2 T, where c_{el} is the electronic specific heat. The dashed line is the weak-coupling BCS behavior (coupling constant $\alpha = 1.76$) for T_c of 2.85 K. The green solid line is the theoretical curve for d-wave pairing on a simple cylindrical Fermi surface with line nodes along the axial direction [98]. Horizontal solid line corresponds to the normal-state electronic specific-heat coefficient γ_N.

structure and superconducting properties of another superconducting doped TCI $(Pb_{0.5}Sn_{0.5})_{1-x}In_xTe$ has been investigated [97]. The single crystal of $(Pb_{0.5}Sn_{0.5})_{1-x}In_xTe$ grown by a modified floating-zone method retains the rocksalt structure up to the solubility limit of In ($x \simeq 0.30$). The dependence of T_c and the upper critical magnetic field (H_{c2}) on the In content x has been measured and the maximum $T_c = 4.7$ K for $x = 0.30$ with $\mu_0 H_{c2}$ ($T = 0$) ~5 T was found. Further studies on the material to find a signature of unconventional superconductivity are necessary to conclude that $(Pb_{0.5}Sn_{0.5})_{1-x}In_xTe$ is a TSC. It is also important to search for other candidates for TSCs based on superconducting doped TCI.

3.3. *Electron-doped natural heterostructure material: $Cu_x(PbSe)_5(Bi_2Se_3)_6$*

Recently, a new SC based on a topological insulator heterostructure material, $Cu_x(PbSe)_5(Bi_2Se_3)_6$ (abbreviated CPSBS), was discovered [99]. The pristine material $(PbSe)_5(Bi_2Se_3)_6$ (PSBS) is a natural heterostructure of a TI (Bi_2Se_3) and an ordinary insulator (PbSe). It was found that the PbSe unit works as a block layer and the topological boundary states are encapsulated in each Bi_2Se_3 unit, making the system to possess quasi-two-dimensional states of topological origin throughout the bulk [100]. CPSBS is synthesized by intercalating Cu into PSBS with post annealing that is essential to activate the superconductivity similar to the activation process of $Cu_xBi_2Se_3$. It is worth noting that the specific-heat behavior of CPSBS suggests for the first time in a TI-based SC that unconventional superconductivity occurs in the bulk with gap nodes as indicated in Fig. 5. The existence of gap nodes in a strongly spin-orbit coupled SC gives rise to spin-split ABSs that are hallmark of topological superconductivity. Hence this new SC emerges as an intriguing candidate for TSCs.

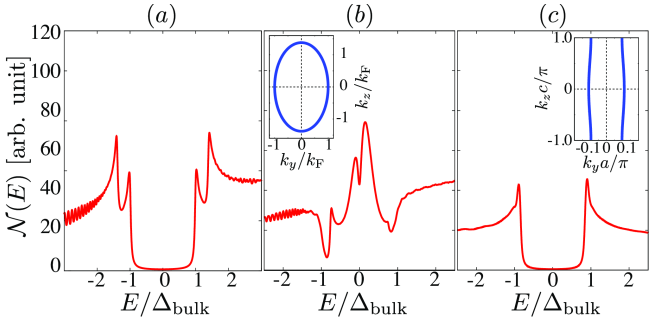

Figure 6: (a) Surface density of states for the bulk s-wave pairing (A_{1g}) at $(\tilde{m}_1, \tilde{m}_2) = (-0.17, -0.20)$. Surface density of states for the A_{1u} state with a spheroidal Fermi surface (b) and a cylindrical shape (c). The insets in (b) and (c) show the Fermi surface, where a and c are the lattice constants.

4. Outlook

4.1. *Pairing symmetry of $Cu_xBi_2Se_3$*

Here, we revisit the pairing symmetry and topological superconductivity of $Cu_xBi_2Se_3$. As shown in Sec. 3.1, surface sensitive experiments observed pronounced ZBCPs on the (111) surface [39, 74, 83], which are strong signatures of bulk topological odd parity superconductivity. On the other hand, conflicting experimental results of conductance and tunneling spectroscopy were recently reported [84, 85, 101], which led to contrary statement that this material has a conventional s-wave pairing symmetry.

First of all, we would like to emphasize that, even if the bulk of $Cu_xBi_2Se_3$ is a conventional s-wave pairing, i.e., the A_{1g} state (Δ_{1a}) in Table 1, the surface structure becomes unconventional [67]. As clarified in Eq. (7), the Dirac fermion is fully polarized in the orbital space, which breaks the inversion symmetry. Since Cooper pairs are equally populated to both orbitals in the A_{1g} state, the orbital polarization of the Dirac fermion strongly suppresses the condensation energy at the surface. As demonstrated in Ref. [67], the mixing of the subdominant component $\Delta_3\sigma_z$, which has the odd parity pairing, is indispensable for the maximum gain of the condensation energy. When the surface Dirac fermions that are remnants of the parent TIs are well defined, therefore, the intertwining with bulk superconductivity gives rise to a large energy gap in the surface Dirac cone, $\Delta_{\rm surf}$. This is distinguishable from the gap in the bulk conduction band, $\Delta_{\rm bulk}$. This results in the double-coherence structure of the surface density of states, as shown in Fig. 2(a). Hence, the bulk conventional even-parity scenario is inconsistent with a simple U-shaped form in the surface density of states reported in Ref. [85] and the STS result in Sec. 3.1 is a puzzle.

A possible scenario for $Cu_xBi_2Se_3$ is bulk odd parity superconductivity with a Fermi surface evolution. For bulk odd parity pairing, no surface parity mixing is induced by Dirac fermions. The surface density of states has a pronounced zero energy peak which is responsible for a ZBCP [55, 58, 59, 60], as shown in Fig. 6(b), when the Fermi surface encloses the Γ point. As discussed in Sec. 2.3, the topological superconductivity and the existence of zero energy density of states on the surface are sensitive to the shape of the Fermi surface. For a cylindrical

Fermi surface which does not enclose the Γ point, the surface state is no longer topologically protected and thus the resultant surface density of states on the (111) surface becomes a simple U-shaped form (Fig. 6(c)). This feature is commonly applicable to the A_{1u} and E_u states.

We would like to notice that the E_u state is the two-dimensional representation and the arbitrary linear combination, $\sigma_y s_x \cos\phi + \sigma_y s_y \sin\phi$, rotates the nodal direction, where ϕ is the azimuthal angle and the nodal direction is denoted by the unit vector $(\sin\phi, \cos\phi)$. Since the point nodes in the E_u state is protected by the mirror reflection symmetry (15) with respect to the *y*-*z* plane, the bulk excitation in the E_u state becomes gapful for $\phi \neq 0$, $\pm\pi/3$, and $\pm 2\pi/3$. Fu [49] recently suggested that in the presence of the extra "warping" term in Eq. (6), the E_u scenario is able to explain all experimental results including both the bulk and surface measurements. The fully gapped E_u state may be energetically competitive to the A_{1u} state.

We also mention that in the presence of a phonon-mediated short-range interaction, bulk odd parity pairing is energetically competitive to even parity pairing (A_{1g}). Brydon *et al.* demonstrated that in addition to the phonon-mediated interaction, a repulsive electron-electron interaction based on the Coulomb pseudopotential is critical to stabilizing the spin-triplet odd-parity states [102]. The bulk odd-parity pairing state, the A_{1u} or fully gapped E_u state, may be stabilized by phonon mechanism in the presence of a weak electron-electron correlation.

Apart from $\boldsymbol{k}$-independent pairing, momentum-dependent pairing was examined in Ref. [103, 104]. Recently, first-principle linear-response calculations predict that a *p*-wave-like state can be favored by a conventional phonon-mediated mechanism [105]. This is attributed to a singular behavior of the electron-phonon interaction at long wavelengths.

4.2. Smoking-gun for topological superconductivity

As discussed in Sec. 4.1, a promising candidate for $Cu_xBi_2Se_3$ is an odd parity pairing, the A_{1u} or E_u state. Since both odd parity pairings have a twisted Majorana cone, they can equally explain a pronounced ZBCP in tunneling spectroscopy. Thus, it is hard to identify the bulk pairing symmetry via point contact measurements. Here, we summarize smoking-gun experiments for identifying bulk pairing symmetry and for extracting properties inherent to topological superconductivity.

Spin susceptibility.— First, the Knight shift in nuclear magnetic resonance experiments can provide a smoking-gun evidence for the spin state of the bulk pairing symmetry [56, 57, 106]. Hashimoto *et al.* [56, 57] introduced the $\boldsymbol{d}$-vector that describes the spin-triplet component of Δ in the band representation. It turns out that the Knight shift in the A_{1u} state is distinguishable from that of the E_u state, when an applied field is rotated within the *ab* plane. The former is characterized by an hedge-hog-like $\boldsymbol{d}$-vector profile in the $\boldsymbol{k}$-space, similarly with that of the BW state in ^{3}He. This is responsible for an isotropic magnetic response. In contrast, the E_u state results in the uniaxial anisotropy of the Knight shift in the *ab* plane. Furthermore, Nagai predicted that nodal structure in the E_u state is detectable through angle-resolved heat capacity and thermal conductivity measurements [107]. In the E_u state, the zero-energy density of states around a vortex core shows twofold rotational symmetry and splits along the nodal direction with increasing energy.

Thermal Hall conductivity.— One of fingerprint experiments for bulk topological superconductivity is the quantized thermal Hall conductivity. The topology of three-dimensional fully gapped SCs with time-reversal symmetry is characterized by the $\mathbb{Z}$ topological number, w_{3d}, as defined in Eq. (10). It has been shown that the thermal Hall conductivity κ_{xy} is quantized in $\mathbb{Z}$ time-reversal invariant TSCs, $\kappa_{xy} = \frac{\pi^2 k_B^2 T}{12h} w_{3d}$, when a small gap is induced in the Majorana cone [108, 109, 110, 111, 112]. Shimizu and Nomura [113] evaluated the thermal Hall conductivity in the A_{1u} state of $Cu_xBi_2Se_3$. They demonstrated that κ_{xy} depends on a time-reversal breaking perturbation which induces a small gap in the Majorana cone and w_{3d} is directly detectable through the thermal Hall conductivity when the small gap is induced by the complex *s*-wave pair potential.

Topological "crystalline" superconductivity.— Topological superconductivity peculiar to nodal SCs, i.e., the E_u state, is unveiled by introducing the combined $\boldsymbol{Z}_2$ symmetry which is composed of the mirror reflection symmetry and time-reversal symmetry (3). The superconducting state retains the mirror symmetry if the gap function $\Delta(\boldsymbol{k})$ is even or odd under the mirror reflection, $M\Delta(\boldsymbol{k})M^{\mathrm{T}} = \pm\Delta(-k_x, k_y, k_z)$. Then, the BdG Hamiltonian $\mathcal{H}_0(\boldsymbol{k})$ preserves the mirror reflection symmetry

$$\mathcal{M}^{\pm}\mathcal{H}(\boldsymbol{k})\mathcal{M}^{\pm\dagger} = \mathcal{H}(-k_x, k_y, k_z), \tag{15}$$

when an external field is absent. The mirror reflection operator $\mathcal{M}^{\pm}$ is defined as $\mathcal{M}^{\pm} = \mathrm{diag}(M, \pm M^*)$.

Once the Zeeman fields, $\boldsymbol{H}$, are applied, the mirror symmetry with respect to the plane parallel to the Zeeman filed is lost and the time-reversal symmetry is explicitly broken, but a combination of them can be still preserved if $\boldsymbol{H} \cdot \hat{\boldsymbol{x}} = 0$. This is because the combination of the mirror reflection and the time-reversal rotates the magnetic field $\boldsymbol{H} \to (-H_x, H_y, H_z)$. Consequently, the Hamiltonian $\mathcal{H}(\boldsymbol{k})$ with $H_x = 0$ holds the following $\boldsymbol{Z}_2$ symmetry,

$$\mathcal{T}\mathcal{M}^{\pm}\mathcal{H}(\boldsymbol{k})\mathcal{M}^{\pm\dagger}\mathcal{T}^{-1} = \mathcal{H}(k_x, -k_y, -k_z). \tag{16}$$

Combining the $\boldsymbol{Z}_2$ symmetry with the particle-hole symmetry, $\mathcal{C}\mathcal{H}_{\mathrm{eff}}(\boldsymbol{k})\mathcal{C}^{-1} = -\mathcal{H}^*_{\mathrm{eff}}(-\boldsymbol{k})$, we define the chiral symmetry operator, $\Gamma_1 = \mathcal{C}\mathcal{T}\mathcal{M}^{\pm}$. Then, it turns out that Γ_1 is anti-commutable with the effective Hamiltonian $\left\{\Gamma_1, \mathcal{H}(0, k_y, k_z)\right\} = 0$. Therefore, similarly to w_{3d} in Eq. (10), the one-dimensional winding number is defined as $w_{1d}(k_y) = -\frac{1}{4\pi i}\int dk_z [\Gamma\mathcal{H}^{-1}(\boldsymbol{k})\partial_{k_z}\mathcal{H}(\boldsymbol{k})]_{k_x=0}$ [24, 114, 115]. From the generalized index theorem in Ref. [114], the non-zero value of w_{1d} is equal to the number of zero energy states that are bound to the surface.

Let us now consider $\Delta = \Delta_{4x}\sigma_y s_x$ in the E_u state, where the point nodes lie in the mirror plane ($\phi = 0$). In this situation, one finds $w_{1d}(k_y) = 2$ for $|k_y| < k_F$, and otherwise $w_{1d}(k_y) = 0$. There appear doubly-degenerate zero energy states along the chiral symmetric plane $k_x = 0$ in the E_u state. Hence, the mirror-symmetry-protected topological invariant ensures the existence of surface Fermi arc that connects two point nodes. Such a surface Fermi arc can also be realized in the planar state of ^{3}He [24] and the E_{1u} scenario of the heavy fermion SC UPt_3 [35] (see Fig. 7).

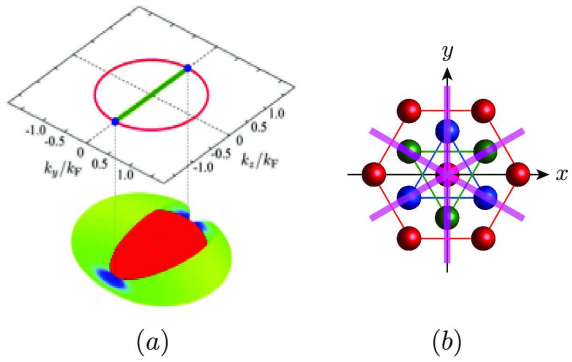

Figure 7: (a) A stereographic view of the energy gap of the E_u state. The Fermi surface and point nodes are projected onto the surface in the $k_x k_y$ plane, where the topologically protected surface Fermi arc connects to two point nodes. (b) Crystal structure of $Cu_xBi_2Se_3$ viewed from the c-axis and three mirror planes.

Now following Refs. [24, 115, 116, 117], one can show that multiple Majorana zero modes with chiral symmetry ensures the Ising character of the topologically protected zero energy states. The topologically protected surface Fermi arc does not contribute to the local density operator, $\rho^{(\mathrm{surf})}(\boldsymbol{r}) = 0$. This indicates that the MFs protected by the chiral symmetry can not be coupled to the local density fluctuations and thus are very robust against non-magnetic impurities. Similarly, the local spin operator, $\boldsymbol{S}$, is constructed from the surface MF as $\boldsymbol{S}^{(\mathrm{surf})} = (S_x, 0, 0)$. This implies that only the surface MF has anisotropic magnetic response. The surface MF and topological Fermi arc are insensitive to a magnetic field along the chiral symmetric plane, but fragile against a field perpendicular to the plane. Since the surface Fermi arc is responsible for a ZBCP, the anisotropic magnetic response of MFs might be observable in point contact experiments when an applied field is rotated within the *ab* plane. The anisotropic magnetic response can be a manifestation of TSCs with the combined $\boldsymbol{Z}_2$ symmetry, i.e., the E_u state with point nodes.

We would like to notice that arbitrary linear combination, $\sigma_y s_x \cos\phi + \sigma_y s_y \sin\phi$, cannot be invariant under the mirror reflection symmetry $M = is_x$, when $\phi \neq 0, \pm\pi/3$, and $\pm 2\pi/3$. As mentioned in Sec. 4.1 and [49], the E_u state without mirror symmetry becomes fully gapped. In this situation, $w_{1\mathrm{d}}$ introduced above is irrelevant and the argument on Majorana Ising spins is not applicable to the E_u state where the nodal direction is tilted from the mirror invariant plane.

Josephson coupling.— The existence of the Majorana cone twisted by the surface Dirac fermions is peculiar to superconducting doped topological materials. It has been predicted [10, 118] that bulk odd parity pairing and surface helical MF are detectable through Josephson currents. In a junction between a *conventional* s-wave and the A_{1u} state of the superconducting doped topological materials, the leading order of the Josephson current $J(\varphi)$ becomes the second-order form, $J(\varphi) \sim \sin 2\varphi$, where φ is the relative phase difference [118]. This is because a s-wave pairing is even under the mirror reflection, while the A_{1u} state is odd as shown in Table 1. In addition, Yamakage *et al.* [118] pointed out that in the junction between superconducting TIs, the Josephson current is highly sensitive to the difference in the spin-helicity of the surface MFs at the interface, where the positive (negative) helicity characterizes the existence of Majorana "cone" ("caldera"). The Josephson current between different helicity is strongly suppressed at low temperatures, which is contrast to that in the junction with same helicity.

5. Summary

The search for Majorana fermion is currently one of the hottest issues in the physics community and various types of promising platforms have been theoretically proposed, as well as experimentally investigated during the last several years. In this review we focused on studies of superconducting doped topological materials that preserve the time-reversal-invariance. We began with a theoretical description of odd-parity pairing systems from a basic concept of symmetry invariances which are important to understand topological superconductors. The normal state of time-reversal-invariant topological superconductors is characterized by the presence of Dirac fermions. We discussed the role of the Dirac fermions in the topological superconductors. To clarify the conditions for realizing topological superconductivity in doped topological materials, topological invariants and possible paring symmetry in the system are denoted. We continued with a summary of studies on the properties of both normal and superconducting states in real existing materials: $Cu_xBi_2Se_3$, $Sn_{1-x}In_xTe$, $(Pb_{0.5}Sn_{0.5})_{1-x}In_xTe$, and $Cu_x(PbSe)_5(Bi_2Se_3)_6$. We found that the recent theoretical developments allow us to consistently interpret controversial results aroused from different experimental methods. In this review, we shed light on the effects of disorder in the system. In particular, we discussed that the observed moderate suppression of T_c of $Cu_xBi_2Se_3$ with increasing the concentration of Cu, which behave as non-magnetic impurities in the superconductor, can be explained by anomalous robustness of superconductivity in the presence of nonmagnetic impurity scattering, which is peculiar to superconducting topological materials. Finally, in order to experimentally identify the existence of Majorana fermions in candidate platforms of topological superconductors, we proposed future experiments to observe the anisotropic magnetic response of the candidate materials, as well as Josephson coupling effects.

We thank A. A. Taskin, D. Derks, Y. Nagai, A. Yamakage, M. Sato, Y. Tanaka, and Y. Ando for fruitful discussions. This work is supported by JPSJ (Grants Nos. 25287085 and 25800199), the "Topological Quantum Phenomena" Grant-in Aid (No. 22103005) for Scientific Research on Innovative Areas from MEXT of Japan, Inamori Foundation, and the Murata Science Foundation.

[1] E. Majorana, Teoria simmetrica dell'elettrone e del positrone, Nuovo Cimento 14 (1937) 171.
[2] F. Wilczek, Majorana returns, Nature Phys. 5 (2009) 614.
[3] X.-L. Qi, S.-C. Zhang, Topological insulators and superconductors, Rev. Mod. Phys. 83 (2011) 1057.
[4] Y. Tanaka, M. Sato, N. Nagaosa, Symmetry and topology in superconductors —odd-frequency pairing and edge states—, J. Phys. Soc. Jpn. 81 (2012) 011013.

[5] M. Sato, S. Fujimoto, Existence of Majorana fermions and topological order in nodal superconductors with spin-orbit interactions in external magnetic fields, Phys. Rev. Lett. 105 (2010) 217001.

[6] A. P. Schnyder, S. Ryu, A. Furusaki, A. W. W. Ludwig, Classification of topological insulators and superconductors in three spatial dimensions, Phys. Rev. B 78 (2008) 195125.

[7] X.-L. Qi, T. L. Hughes, S. Raghu, S.-C. Zhang, Time-reversal-invariant topological superconductors and superfluids in two and three dimensions, Phys. Rev. Lett. 102 (2009) 187001.

[8] X.-L. Qi, T. L. Hughes, S.-C. Zhang, Chiral topological superconductor from the quantum hall state, Phys. Rev. B 82 (2010) 184516.

[9] M. Sato, Topological properties of spin-triplet superconductors and fermi surface topology in the normal state, Phys. Rev. B 79 (2009) 214526.

[10] L. Fu, E. Berg, Odd-parity topological superconductors: Theory and application to $Cu_xBi_2Se_3$, Phys. Rev. Lett. 105 (2010) 097001.

[11] M. Sato, Topological odd-parity superconductors, Phys. Rev. B 81 (2010) 220504(R).

[12] L. Fu, C. L. Kane, Superconducting proximity effect and Majorana fermions at the surface of a topological insulator, Phys. Rev. Lett. 100 (2008) 096407.

[13] L. Fu, C. L. Kane, Probing neutral Majorana fermion edge modes with charge transport, Phys. Rev. Lett. 102 (2009) 216403.

[14] J. Alicea, New directions in the pursuit of Majorana fermions in solid state systems, Rep. Prog. Phys. 75 (7) (2012) 076501.

[15] C. W. Beenakker, Search for Majorana fermions in superconductors, Annu. Rev. Condens. Mat. Phys. 4 (2013) 113.

[16] J. D. Sau, R. M. Lutchyn, S. Tewari, S. Das Sarma, Generic new platform for topological quantum computation using semiconductor heterostructures, Phys. Rev. Lett. 104 (2010) 040502.

[17] M. Sato, S. Fujimoto, Topological phases of noncentrosymmetric superconductors: Edge states, Majorana fermions, and non-Abelian statistics, Phys. Rev. B 79 (2009) 094504.

[18] M. Sato, Y. Takahashi, S. Fujimoto, Non-Abelian topological order in *s*-wave superfluids of ultracold fermionic atoms, Phys. Rev. Lett. 103 (2009) 020401.

[19] M. Sato, Y. Takahashi, S. Fujimoto, Non-Abelian topological orders and Majorana fermions in spin-singlet superconductors, Phys. Rev. B 82 (2010) 134521.

[20] A. R. Akhmerov, J. Nilsson, C. W. J. Beenakker, Electrically detected interferometry of Majorana fermions in a topological insulator, Phys. Rev. Lett. 102 (2009) 216404.

[21] Y. Tanaka, T. Yokoyama, N. Nagaosa, Manipulation of the Majorana fermion, Andreev reflection, and Josephson current on topological insulators, Phys. Rev. Lett. 103 (2009) 107002.

[22] L. Fu, Electron teleportation via Majorana bound states in a mesoscopic superconductor, Phys. Rev. Lett. 104 (2010) 056402.

[23] T. Mizushima, M. Ichioka, K. Machida, Role of the Majorana fermion and the edge mode in chiral superfluidity near a *p*-wave feshbach resonance, Phys. Rev. Lett. 101 (2008) 150409.

[24] T. Mizushima, Y. Tsutsumi, M. Sato, K. Machida, Symmetry protected topological superfluid 3 he-b, J. Phys.: Condens. Matter 27 (2015) 113203.

[25] M. Silaev, G. Volovik, Andreev-majorana bound states in superfluids, J. Exp. Theor. Phys. 119 (2014) 1042.

[26] J. Klinovaja, D. Loss, Time-reversal invariant parafermions in interacting rashba nanowires, Phys. Rev. B 90 (2014) 045118.

[27] J. Klinovaja, A. Yacoby, D. Loss, Kramers pairs of majorana fermions and parafermions in fractional topological insulators, Phys. Rev. B 90 (2014) 155447.

[28] K. Michaeli, L. Fu, Spin-orbit locking as a protection mechanism of the odd-parity superconducting state against disorder, Phys. Rev. Lett. 109 (2012) 187003.

[29] M. S. Foster, H.-Y. Xie, Y.-Z. Chou, Topological protection, disorder, and interactions: Survival at the surface of three-dimensional topological superconductors, Phys. Rev. B 89 (2014) 155140.

[30] Y. Nagai, Y. Ota, M. Machida, Nonmagnetic impurity effects in a three-dimensional topological superconductor: From *p*- to *s*-wave behaviors, Phys. Rev. B 89 (2014) 214506.

[31] Y. Nagai, Robust superconductivity with nodes in the superconducting topological insulator $Cu_xBi_2Se_3$: Zeeman orbital field and nonmagnetic impurities, Phys. Rev. B 91 (2015) 060502(R).

[32] G. E. Volovik, *The Universe in a Helium Droplet* (Oxford University Press, Oxford, 2003).

[33] M. Sato, A. Yamakage, T. Mizushima, Mirror Majorana zero modes in spinful superconductors/superfluids non-Abelian anyons in integer quantum vortices, Physica E 55 (2014) 20.

[34] Y. Ueno, A. Yamakage, Y. Tanaka, M. Sato, Symmetry-protected Majorana fermions in topological crystalline superconductors: Theory and application to Sr_2RuO_4, Phys. Rev. Lett. 111 (2013) 087002.

[35] Y. Tsutsumi, M. Ishikawa, T. Kawakami, T. Mizushima, M. Sato, M. Ichioka, K. Machida, Upt_3 as a topological crystalline superconductor, J. Phys. Soc. Jpn. 82 (2013) 113707.

[36] J. A. Sauls, The order parameter for the superconducting phases of UPt_3, Adv. Phys. 43 (1994) 113.

[37] R. Joynt, L. Taillefer, The superconducting phases of UPt_3, Rev. Mod. Phys. 74 (2002) 235.

[38] P. Goswami, A. H. Nevidomskyy, Double Berry monopoles and topological surface states in the superconducting B-phase of UPt_3. `arXiv:1403.0924`.

[39] S. Sasaki, M. Kriener, K. Segawa, K. Yada, Y. Tanaka, M. Sato, Y. Ando, Topological superconductivity in $Cu_xBi_2Se_3$, Phys. Rev. Lett. 107 (2011) 217001.

[40] L. Fu, C. L. Kane, Topological insulators with inversion symmetry, Phys. Rev. B 76 (2007) 045302.

[41] S. Murakami, N. Nagaosa, S.-C. Zhang, Dissipationless quantum spin current at room temperature, Science 301 (2003) 1348.

[42] S. Murakami, N. Nagosa, S.-C. Zhang, SU(2) non-Abelian holonomy and dissipationless spin current in semiconductors, Phys. Rev. B 69 (2004) 235206.

[43] H. Zhang, C.-X. Liu, X.-L. Qi, X. Dai, Z. Fang, S.-C. Zhang, Topological insulators in Bi_2Se_3, Bi_2Te_3 and Sb_2Te_3 with a single Dirac cone on the surface, Nat. Phys. 5 (2009) 438.

[44] C.-X. Liu, X.-L. Qi, H. Zhang, X. Dai, Z. Fang, S.-C. Zhang, Model hamiltonian for topological insulators, Phys. Rev. B 82 (2010) 045122.

[45] D. L. Mitchell, R. F. Wallis, Theoretical energy-band parameters for the lead salts, Phys. Rev. 151 (1966) 581.

[46] T. H. Hsieh, H. Lin, J. Liu, W. Duan, A. Bansil, L. Fu, Topological crystalline insulators in the SnTe material class, Nat. Commun. 3 (2012) 982.

[47] J. Liu, W. Duan, L. Fu, Two types of surface states in topological crystalline insulators, Phys. Rev. B 88 (2013) 241303.

[48] L. Fu, Hexagonal warping effects in the surface states of the topological insulator Bi_2Te_3, Phys. Rev. Lett. 103 (2009) 266801.

[49] L. Fu, Odd-parity topological superconductor with nematic order: Application to $Cu_xBi_2Se_3$, Phys. Rev. B 90 (2014) 100509.

[50] Y. Ando, Topological insulator materials, J. Phys. Soc. Jpn. 82 (10) (2013) 102001.

[51] L. Fu, Topological crystalline insulators, Phys. Rev. Lett. 106 (2011) 106802.

[52] S. Ryu, A. P. Schnyder, A. Furusaki, A. W. W. Ludwig, Topological insulators and superconductors: tenfold way and dimensional hierarchy, New J. Phys. 12 (2010) 065010.

[53] G. Volovik, Topological invariant for superfluid 3He-B and quantum phase transitions, JETP Lett. 90 (2009) 587.

[54] G. Volovik, Fermion zero modes at the boundary of superfluid 3He-B, JETP Lett. 90 (2009) 398.

[55] A. Yamakage, K. Yada, M. Sato, Y. Tanaka, Theory of tunneling conductance and surface-state transition in superconducting topological insulators, Phys. Rev. B 85 (2012) 180509.

[56] T. Hashimoto, K. Yada, A. Yamakage, M. Sato, Y. Tanaka, Bulk electronic state of superconducting topological insulator, J. Phys. Soc. Jpn. 82 (2013) 044704.

[57] T. Hashimoto, K. Yada, A. Yamakage, M. Sato, Y. Tanaka, Effect of fermi surface evolution on superconducting gap in superconducting topological insulator, Superconductor Science and Technology 27 (2014) 104002.

[58] L. Hao, T. K. Lee, Surface spectral function in the superconducting state of a topological insulator, Phys. Rev. B 83 (2011) 134516.

[59] T. H. Hsieh, L. Fu, Majorana fermions and exotic surface Andreev bound states in topological superconductors: Application to $Cu_xBi_2Se_3$, Phys. Rev. Lett. 108 (2012) 107005.

[60] S. Takami, K. Yada, A. Yamakage, M. Sato, Y. Tanaka, Quasi-classical theory of tunneling spectroscopy in superconducting topological insulator, J. Phys. Soc. Jpn. 83 (2014) 064705.

[61] S.-K. Yip, Models of superconducting Cu:Bi_2Se_3: Single- versus two-band description, Phys. Rev. B 87 (2013) 104505.

[62] Y. Tanaka, S. Kashiwaya, Theory of tunneling spectroscopy of *d*-wave superconductors, Phys. Rev. Lett. 74 (1995) 3451.

[63] S. Kashiwaya, Y. Tanaka, Tunnelling effects on surface bound states in unconventional superconductors, Rep. Prog. Phys. 63 (2000) 1641.

[64] Y. Asano, Y. Tanaka, Y. Matsuda, S. Kashiwaya, A theoretical study of tunneling conductance in $PrOs_4Sb_{12}$ superconducting junctions, Phys. Rev. B 68 (2003) 184506.

[65] L. A. Wray, S.-Y. Xu, Y. Xia, Y. S. Hor, D. Qian, A. V. Fedorov, H. Lin, A. Bansil, R. J. Cava, M. Z. Hasan, Observation of topological order in a superconducting doped topological insulator, Nat. Phys. 6 (2010) 855.

[66] Y. Nagai, H. Nakamura, M. Machida, Inhomogeneity effects in topological superconductors, JPS Conf. Proc. 3 (2014) 015013.

[67] T. Mizushima, A. Yamakage, M. Sato, Y. Tanaka, Dirac-frmion-induced parity mixing in superconducting topological insulators, Phys. Rev. B 90 (2014) 184516.

[68] P. Anderson, Theory of dirty superconductors, J. Phys. Chem. of Solids 11 (1959) 26.

[69] M. Kriener, K. Segawa, Z. Ren, S. Sasaki, Y. Ando, Bulk superconducting phase with a full energy gap in the doped topological insulator $Cu_xBi_2Se_3$, Phys. Rev. Lett. 106 (2011) 127004.

[70] Y. S. Hor, A. J. Williams, J. G. Checkelsky, P. Roushan, J. Seo, Q. Xu, H. W. Zandbergen, A. Yazdani, N. P. Ong, R. J. Cava, Superconductivity in $Cu_xBi_2Se_3$ and its implications for pairing in the undoped topological insulator, Phys. Rev. Lett. 104 (2010) 057001.

[71] M. Kriener, K. Segawa, Z. Ren, S. Sasaki, S. Wada, S. Kuwabata, Y. Ando, Electrochemical synthesis and superconducting phase diagram of $Cu_xBi_2Se_3$, Phys. Rev. B 84 (2011) 054513.

[72] B. J. Lawson, Y. S. Hor, L. Li, Quantum oscillations in the topological superconductor candidate $Cu_{0.25}Bi_2Se_3$, Phys. Rev. Lett. 109 (2012) 226406.

[73] R. Kondo, T. Yoshinaka, Y. Imai, A. Maeda, Reproducible synthetic method for the topological superconductor $Cu_xBi_2Se_3$, J. Phys. Soc. Jpn. 82 (2013) 063702.

[74] T. Kirzhner, E. Lahoud, K. B. Chaska, Z. Salman, A. Kanigel, Point-contact spectroscopy of $Cu_{0.2}Bi_2Se_3$ single crystals, Phys. Rev. B 86 (2012) 064517.

[75] B. Balian, N. R. Werthamer, Superconductivity with pairs in a relative *p* wave, Phys. Rev. 131 (1963) 1553.

[76] A. I. Larkin, Vector pairing in superconductors of small dimensions, JETP Lett. 2 (1965) 130.

[77] Y. Maeno, S. Kittaka, T. Nomura, S. Yonezawa, K. Ishida, Evaluation of spin-triplet superconductivity in Sr_2RuO_4, J. Phys. Soc. Jpn. 81 (2012) 011009.

[78] M. Kriener, K. Segawa, S. Sasaki, Y. Ando, Anomalous suppression of the superfluid density in the $Cu_xBi_2Se_3$ superconductor upon progressive cu intercalation, Phys. Rev. B 86 (2012) 180505(R).

[79] L. J. Sandilands, A. A. Reijnders, M. Kriener, k. Segawa, S. Sasaki, Y. Ando, Doping-dependent charge dynamics in $Cu_xBi_2Se_3$, Phys. Rev. B 90 (2014) 094503.

[80] S. Kashiwaya, H. Kashiwaya, H. Kambara, T. Furuta, H. Yaguchi, Y. Tanaka, Y. Maeno, Edge states of Sr_2RuO_4 detected by in-plane tunneling spectroscopy, Phys. Rev. Lett. 107 (2011) 077003.

[81] D. Daghero, R. S. Gonnelli, Probing multiband superconductivity by point-contact spectroscopy, Supercond. Sci. Technol. 23 (2010) 043001.

[82] D. C. Ralph, C. T. Black, M. Tinkham, Spectroscopic measurements of discrete electronic states in single metal particles, Phys. Rev. Lett. 74 (1995) 3241.

[83] X. Chen, C. Huan, Y. S. Hor, C. A. R. Sá de Melo, Z. Jiang, Point-contact Andreev reflection spectroscopy of candidate topological superconductor $Cu_{0.25}Bi_2Se_3$. `arXiv:1210.6054`.

[84] H. Peng, D. De, B. Lv, F. Wei, C.-W. Chu, Absence of zero-energy surface bound states in $cu_xbi_2se_3$ studied via Andreev reflection spectroscopy, Phys. Rev. B 88 (2013) 024515.

[85] N. Levy, T. Zhang, J. Ha, F. Sharifi, A. A. Talin, Y. Kuk, J. A. Stroscio, Experimental evidence for *s*-wave pairing symmetry in superconducting $cu_xbi_2se_3$ single crystals using a scanning tunneling microscope, Phys. Rev. Lett. 110 (2013) 117001.

[86] E. Lahoud, E. Maniv, M. S. Petrushevsky, M. Naamneh, S. Ribak, A. Wiedmann, L. Petaccia, Z. Salmn, K. B. Chashka, Y. Dagan, A. Kanigel, Evolution of the fermi surface of a doped topological insulator with carrier concentration, Phys. Rev. B 88 (2013) 195107.

[87] T. V. Bay, T. Naka, Y. K. Huang, H. Luigjes, M. S. Golden, A. de Visser, Superconductivity in the doped topological insulator $Cu_xBi_2Se_3$ under high pressure, Phys. Rev. Lett. 108 (2012) 057001.

[88] A. S. Erickson, J.-H. Chu, M. F. Toney, T. H. Geballe, I. R. Fisher, Enhanced superconducting pairing interaction in indium-doped tin telluride, Phys. Rev. B 79 (2009) 024520.

[89] S. Sasaki, Z. Ren, A. A. Taskin, K. Segawa, L. Fu, Y. Ando, Odd-parity pairing and topological superconductivity in a strongly spin-orbit coupled semiconductor, Phys. Rev. Lett. 109 (2012) 217004.

[90] S. Sasaki, Y. Ando, Superconducting $Sn_{1-x}In_xTe$ nanoplates. `arXiv:1410.4852`.

[91] J. K. Hulm, C. K. Jones, D. W. Deis, H. A. Fairbank, P. A. Lawless, Superconducting interactions in tin telluride, Phys. Rev. 169 (1968) 388.

[92] T. Sato, Y. Tanaka, K. Nakayama, S. Souma, T. Takahashi, S. Sasaki, Z. Ren, A. A. Taskin, K. Segawa, Y. Ando, Fermiology of the strongly spin-orbit coupled superconductor $Sn_{1-x}In_xTe$: Implications for topological superconductivity, Phys. Rev. Lett. 110 (2013) 206804.

[93] R. D. Zhong, J. A. Schneeloch, X. Y. Shi, Z. J. Xu, C. Zhang, J. M. Tranquada, G. D. Gu, Optimizing the superconducting transition temperature and upper critical field of $Sn_{1-x}In_xTe$, Phys. Rev. B 88 (2013) 020505(R).

[94] M. Saghir, J. A. T. Barker, G. Balakrishnan, A. D. Hillier, M. R. Lees, Superconducting properties of $Sn_{1-x}In_xTe$ ($x = 0.38 - 0.45$) studied using muon-spin spectroscopy, Phys. Rev. B 90 (2014) 064508.

[95] G. Balakrishnan, L. Bawden, S. Cavendish, M. R. Lees, Superconducting properties of the in-substituted topological crystalline insulator SnTe, Phys. Rev. B 87 (2013) 140507(R).

[96] M. Novak, S. Sasaki, M. Kriener, K. Segawa, Y. Ando, Unusual nature of fully gapped superconductivity in in-doped SnTe, Phys. Rev. B 88 (2013) 140502.

[97] R. D. Zhong, J. A. Schneeloch, T. S. Liu, F. E. Camion, J. M. Tranquada, G. D. Gu, Superconductivity induced by in substitution into the topological crystalline insulator $Pb_{0.5}Sn_{0.5}Te$, Phys. Rev. B 90 (2014) 020505(R).

[98] H. Won, K. Maki, *d*-wave superconductor as a model of high-T_c superconductors, Phys. Rev. B 49 (11994) 1397.

[99] S. Sasaki, K. Segawa, Y. Ando, Superconductor derived from topological insulator heterostructure, Phys. Rev. B 90 (2014) 220504(R).

[100] K. Nakayama, K. Eto, Y. Tanaka, T. Sato, S. Souma, T. Takahashi, K. Segawa, Y. Ando, Manipulation of topological states and the bulk band gap using natural heterostructures of a topological insulator, Phys. Rev. Lett. 109 (2012) 236804.

[101] As mentioned in Sec.3.1, both unconventional ZBCP and conventional Blonder-Tinkham-Klapwijk (BTK) spectra were obsereved in Ref. [74].

[102] P. M. R. Brydon, S. D. Sarma, H.-Y. Hui, J. D. Sau, Odd-parity superconductivity from phonon-mediated pairing: Application to $Cu_xBi_2Se_3$, Phys. Rev. B 90 (2014) 184512.

[103] L. Hao, G.-L. Wang, T.-K. Lee, J. Wang, W.-F. Tsai, Y.-H. Yang, Anisotropic spin-singlet pairings in $Cu_xBi_2Se_3$ and Bi_2Te_3, Phys. Rev. B 89 (2014) 214505.

[104] L. Chen, S. Wan, Surface spectral function of momentum-dependent pairing potentials in a topological insulator: application to $Cu_xBi_2Se_3$, J. of Phys.: Condens. Matter 25 (2013) 215702.

[105] X. Wan, S. Y. Savrasov, Turning a band insulator into an exotic superconductor, Nat. Commun. 5 (2014) 4144.

[106] B. Zocher, B. Rosenow, Surface states and local spin susceptibility in doped three-dimensional topological insulators with odd-parity superconducting pairing symmetry, Phys. Rev. B 87 (2013) 155138.

[107] Y. Nagai, Field-angle-dependent low-energy excitations around a vortex in the superconducting topological insulator $Cu_xBi_2Se_3$, J. Phys. Soc. Jpn. 83 (2014) 063705.

[108] Z. Wang, X.-L. Qi, S.-C. Zhang, Topological field theory and thermal responses of interacting topological superconductors, Phys. Rev. B 84 (2011) 014527.

[109] S. Ryu, J. E. Moore, A. W. W. Ludwig, Electromagnetic and gravitational responses and anomalies in topological insulators and supercon-

ductors, Phys. Rev. B 85 (2012) 045104.
[110] K. Nomura, S. Ryu, A. Furusaki, N. Nagaosa, Cross-correlated responses of topological superconductors and superfluids, Phys. Rev. Lett. 108 (2012) 026802.
[111] K. Shiozaki, S. Fujimoto, Electromagnetic and thermal responses of z topological insulators and superconductors in odd spatial dimensions, Phys. Rev. Lett. 110 (2013) 076804.
[112] K. Shiozaki, S. Fujimoto, Dynamical axion in topological superconductors and superfluids, Phys. Rev. B 89 (2014) 054506.
[113] Y. Shimizu, K. Nomura, Quantum thermal hall effect of Majorana fermions on the surface of superconducting topoloigcal insulators. arXiv:1403.1021.
[114] M. Sato, Y. Tanaka, K. Yada, T. Yokoyama, Topology of Andreev bound states with flat dispersion, Phys. Rev. B 83 (2011) 224511.
[115] T. Mizushima, M. Sato, K. Machida, Symmetry protected topological order and spin susceptibility in superfluid 3He-B, Phys. Rev. Lett. 109 (2012) 165301.
[116] T. Mizushima, M. Sato, Topological phases of quasi-one-dimensional fermionic atoms with a synthetic gauge field, New J. Phys. 15 (2013) 075010.
[117] K. Shiozaki, M. Sato, Topology of crystalline insulators and superconductors, Phys. Rev. B 90 (2014) 165114.
[118] A. Yamakage, M. Sato, K. Yada, S. Kashiwaya, Y. Tanaka, Anomalous Josephson current in superconducting topological insulator, Phys. Rev. B 87 (2013) 100510.